Acta Crystallographica Section D
Biological Crystallography
ISSN 0907-4449

Crystal structure reveals two alternative conformations in the active site of ribonuclease Sa2

Jozef Ševčík,[a]* Zbigniew Dauter[b] and Keith S. Wilson[c]

[a]Institute of Molecular Biology, Member of the Centre of Excellence for Molecular Medicine, Slovak Academy of Sciences, Dubravska Cesta 21, 84551 Bratislava, Slovak Republic, [b]Synchrotron Radiation Research Section, Macromolecular Crystallography Laboratory, NCI, Brookhaven National Laboratory, Building 757A-X9, Upton, NY 11973, USA, and [c]Structural Biology Laboratory, University of York, York YO10 5YW, England

Correspondence e-mail: jozef.sevcik@savba.sk

Received 18 November 2003
Accepted 15 April 2004

PDB References:
ribonuclease Sa2, form I, 1py3, r1py3sf; form II, 1pyl, r1pylsf.

Three different strains of *Streptomyces aureofaciens* produce the homologous ribonucleases Sa, Sa2 and Sa3. The crystal structures of ribonuclease Sa (RNase Sa) and its complexes with mononucleotides have previously been reported at high resolution. Here, the structures of two crystal forms (I and II) of ribonuclease Sa2 (RNase Sa2) are presented at 1.8 and 1.5 Å resolution. The structures were determined by molecular replacement using the coordinates of RNase Sa as a search model and were refined to R factors of 17.5 and 15.0% and $R_{\rm free}$ factors of 21.8 and 17.2%, respectively. The asymmetric unit of crystal form I contains three enzyme molecules, two of which have similar structures to those seen for ribonuclease Sa, with Tyr87 at the bottom of their active sites. In the third molecule, Tyr87 has moved substantially: the CA atom moves almost 5 Å and the OH of the side chain moves 10 Å, inserting itself into the active site of a neighbouring molecule at a similar position to that observed for the nucleotide base in RNase Sa complexes. The asymmetric unit of crystal form II contains two Sa2 molecules, both of which are similar to the usual Sa structures. In one molecule, two main-chain conformations were modelled in the α-helix. Finally, a brief comparison is made between the conformations of the Sa2 molecules and those of 34 independent molecules taken from 20 structures of ribonuclease Sa and two independent molecules taken from two structures of ribonuclease Sa3 in various crystal forms.

1. Introduction

Streptomyces aureofaciens ribonucleases (RNases Sa, Sa2 and Sa3) are guanylate endoribonucleases that highly specifically hydrolyse the phosphodiester bonds of RNA at the 3′-side of guanosine nucleotides. These enzymes belong to the prokaryotic subgroup of microbial ribonucleases. In spite of a relatively high identity in their primary sequences and their apparently identical specificities and function, several physicochemical properties (isoelectric point, activity, thermal stability) differ substantially between the three proteins. In addition, RNase Sa3 possesses cytotoxic activity against human erythroleukaemia cells (Ševčík, Urbanikova *et al.*, 2002), which is not observed for the other two enzymes but has been reported for some other ribonucleases (for a review, see Leland & Raines, 2001).

The most thoroughly studied *Streptomyces* ribonuclease is RNase Sa. The structures of the enzyme and its complexes with guanosine-3′-monophosphate (3′-GMP; Sevcik *et al.*, 1991), guanosine-2′-monophosphate (2′-GMP; Sevcik, Hill *et al.*, 1993) and guanosine-2′,3′-cyclophosphorothioate (Sevcik, Zegers *et al.*, 1993) have been determined at high resolution. The structure of the free enzyme has been refined at 1.2 Å

resolution (Sevcik *et al.*, 1996) and subsequently at 1.0 Å resolution (Ševčík, Lamzin *et al.*, 2002).

RNase Sa2 consists of 97 amino-acid residues and is highly homologous to RNase Sa, with 54 identical residues (Fig. 1). All residues that differ between these two sequences lie on the surface of the molecule and it is thus not surprising that the structure of RNase Sa2, the main structural features of which are an α-helix (residues 15–26), a three-stranded antiparallel β-sheet (residues 55–59, 70–75, 79–84) and the main-chain segment 42–44 that forms the substrate-binding site, is very similar to that of RNase Sa. In the present paper, the structure of RNase Sa2 is described in two crystal forms (I and II). The Sa2 structures are overlapped with those of Sa and Sa3 and the variation in their conformation is discussed.

2. Experimental

2.1. Isolation and crystallization

The isolation of *S. aureofaciens* ribonucleases is a tedious procedure and the yields are very low. Attempts to overexpress their genes failed in several systems owing to the high toxicity of the enzymes towards the host cells. It was found that barstar, a protein inhibitor of barnase isolated from *Bacillus amyloliquefaciens*, also inhibits *S. aureofaciens* ribonucleases. Contemporary expression of the genes of Sa ribonucleases and the inhibitor barstar eliminates the toxicity (Hartley *et al.*, 1996) and enables yields of up to 80 mg of recombinant protein per litre of cultivation media from *Escherichia coli* (Hebert *et al.*, 1997). The enzyme was prepared according to the procedure described in the latter publication.

Crystal form I of RNase Sa2 was prepared by vapour diffusion from a solution of 1.0% protein by weight in 0.1 *M* phosphate buffer at pH 7.2 and room temperature, with 40% saturated ammonium sulfate as precipitant. Ammonium sulfate lowered the pH in the drops by about 0.5, which was compensated by adding a few drops of ammonia to the reservoir solution. The crystals are monoclinic, space group *C*2, with unit-cell parameters $a = 102.3$, $b = 68.7$, $c = 57.5$ Å, $\beta = 100.4^\circ$. Form I crystals took up to three months to grow to a maximum dimension of about 0.4 mm.

With the aim of increasing the resolution and accuracy of the structure, the enzyme was later crystallized again under the same conditions. While these crystals (form II) were again monoclinic in space group *C*2, the unit-cell parameters were different: $a = 85.0$, $b = 34.1$, $c = 72.3$ Å, $\beta = 109.5^\circ$. The reason for the appearance of two different crystal forms is assumed to be small variations in the experimental conditions.

2.2. Data collection

Data from crystal form I were collected at room temperature from a single crystal on the EMBL X31 beamline at the DORIS storage ring, DESY, Hamburg with a MAR Research (Hamburg) imaging-plate scanner of 180 mm diameter and radiation of wavelength 0.9185 Å. Two sets of images with limiting resolution 1.8 and 2.5 Å were measured, with an oscillation range of 1.5 and 2.0° per image, respectively. For both sets a total rotation of about 140° was covered. For the 'low-resolution' pass the exposure time was diminished tenfold.

Table 1
Data-collection statistics.

Values in parentheses refer to the highest resolution shell.

	Form I	Form II
X-ray source	EMBL-Hamburg, beamline X31	University of York, Cu $K\alpha$
Wavelength (Å)	0.9185	1.5418
Temperature (K)	293	293
Resolution range (Å)	15.0–1.8 (1.83–1.8)	25.0–1.5 (1.53–1.50)
Space group	*C*2	*C*2
Unit-cell parameters		
a (Å)	102.3	85.0
b (Å)	68.7	34.15
c (Å)	57.5	73.3
β (°)	100.4	109.5
Unique reflections	34158 (1796)	29668 (975)
Completeness (%)	99.2 (98.4)	98.6 (90.2)
$R(I)_{\rm merge}$† (%)	5.2 (37.8)	6.3 (27.2)
$I/\sigma(I)$	20.5 (2.9)	22.4 (2.6)

† $R(I)_{\rm merge} = \sum_h \sum_i |I_i - \langle I \rangle| / \sum_h \sum_i I_i$.

X-ray data from crystal form II were collected in-house in York to 1.5 Å resolution at room temperature using a Rigaku rotating-anode generator with Cu $K\alpha$ radiation. Both data sets were processed with *DENZO* and *SCALEPACK* (Otwinowski & Minor, 1997). Data-collection statistics for both crystal forms are shown in Table 1.

2.3. Structure determination

All subsequent calculations were performed with programs from the *CCP*4 package (Collaborative Computational Project, Number 4, 1994) unless otherwise indicated. Crystal form I was solved by molecular replacement with the program *AMoRe* (Navaza, 1994) using RNase Sa (PDB code 1rgg) as the search model. Both the rotation and translation-function searches resulted in three clear solutions. Rigid-body refinement of the resulting model gave a correlation coefficient of

```
Sa      D -VSGTVCLSA LPPEATDTLN LIASDGPFPY SQDGVVFQNR
Sa2    AD PALADVCRTK LPSQAQDTLA LIAKNGPYPY NRDGVVFENR
Sa3   ASV KAVGRVCYSA LPSQAHDTLD LIDEGGPFPY SQDGVVFQNR

Sa        ESVLPTQSYG YYHEYTVITP GARTRGTRRI ITGEATQEDY
Sa2       ESRLPKKGNG YYHEFTVVTP GSNDRGTRRV VTGGY-GEQY
Sa3       EGLLPAHSTG YYHEYTVITP GSPTRGARRI ITGQQWQEDY

Sa        YTGDHYATFS LIDQTC
Sa2       WSPDHYATFQ EIDPRC
Sa3       YTADHYASFR RVDFAC
```

Figure 1
Alignment of the amino-acid sequences of RNase Sa (96 residues), Sa2 (97 residues) and Sa3 (99 residues). Identical residues in Sa and Sa2 are shown in bold (52%).

Table 2
Refinement statistics.

	Form I	Form II
Molecules in AU	3	2
Model-atom sites	769/755/727	787/789
Solvent molecules	277	171
SO_4^{2-}	1	4
R_{free} (%)	21.8	17.2
R (%)	17.5	15.0
Average B values (Å^2)		
Protein atoms	24.8/32.4/33.5	23.2/26.2
Solvent molecules	41.7	40.9
SO_4^{2-} anions	47.5	32.8
Wilson plot (Å^2)	23.2	24.4
Coordinates ESU based on R/R_{free} (Å)	0.15/0.11	0.08/0.06
Stereochemical restraints, r.m.s. (σ)		
Bond distances (Å)	0.021 (0.021)	0.014 (0.021)
Bond angles (°)	1.832 (1.946)	1.540 (1.952)
Chiral centres (Å^3)	1.123 (0.200)	0.099 (0.200)
Planar groups (Å)	0.009 (0.020)	0.007 (0.020)
B-factor restraints		
Main-chain bond (Å^2)	2.05 (1.50)	1.61 (1.50)
Main-chain angle (Å^2)	3.23 (2.00)	2.65 (2.00)
Side-chain bond (Å^2)	4.18 (3.00)	3.51 (3.00)
Side-chain angle (Å^2)	6.33 (4.50)	5.18 (4.50)

54% and an R factor of 42% in the 10–3.5 Å resolution range. The presence of three molecules of Sa2 with a molecular weight of 10 894 Da each gave a V_M parameter of 3.0 Å^3 Da^{-1} and a solvent content of 59% (Matthews, 1968).

Crystal form II was solved by molecular replacement using the form I molecule *A* coordinates as the search model. The structure contains two RNase Sa2 molecules in the asymmetric unit, V_M = 2.1 Å^3 Da^{-1}, with a solvent content of 40%. The tighter packing probably explains the higher resolution attainable for form II is spite of the use of a weaker X-ray source.

2.4. Refinement

Refinement of both structures was carried out using version 5.1.24 of the maximum-likelihood program *REFMAC* (Murshudov *et al.*, 1997) against 95% of the data. The remaining 5% of randomly excluded reflections were used for cross-validation by means of the R_{free} factor (Brünger, 1993). Both structures were refined with isotropic and, in the later stages, with anisotropic temperature factors including the contributions of the H atoms generated at their riding positions on their parent C, N and O atoms. For form I (resolution 1.8 Å), the introduction of H atoms and anisotropic temperature factors lowered R from 20.3 to 17.7% and R_{free} from 23.7 to 22.4% after five refinement cycles. Isotropic and anisotropic temperature factors, bond lengths and bond angles were restrained according to the standard criteria employed in *REFMAC*. After each refinement cycle the automated refinement procedure *ARP*/*wARP* (Perrakis *et al.*, 1999) was applied for modelling and updating the solvent structure. The models were adjusted manually between refinement cycles on the basis of $(3F_o - 2F_c, \alpha_c)$ and $(F_o - F_c, \alpha_c)$ maps using the programs *O* (Jones, 1978) and *XtalView* (McRee, 1993). The final refinement statistics are shown in Table 2.

Table 3
Overlap of form I (A, B, C) and form II (A', B') molecules.

	Form I			Form II	Form I–form II					
	A–*B*	*A*–*C*	*B*–*C*	*A*′–*B*′	*A*′–*A*	*A*′–*B*	*A*′–*C*	*B*′–*A*	*B*′–*B*	*B*′–*C*
R.m.s.d. (Å)	0.32	0.86	0.78	0.32	0.47	0.40	0.86	0.40	0.44	0.86
Max. (Å)	1.24	4.96	4.43	1.24	2.82	1.37	4.80	1.34	1.53	4.76
Position	Ala4	Tyr87	Tyr87	Ala4	Ala4	Ala4	Tyr87	Ala4	Gln18	Tyr87

2.5. Superposition of Sa, Sa2 and Sa3 structures

Form I molecule *A* was chosen as a reference for superposition with the remaining Sa2 molecules and with 34 independent molecules from 20 crystal structures of Sa (the structures of some of the mutants have not yet been deposited in the PDB) and two molecules from two Sa3 structures determined in this laboratory using the program *LSQKAB* from the *CCP*4 suite. Superposition was based on the positions of 89 equivalent CA atoms. CA atoms which were not determined in at least one of the molecules were excluded from all molecules in the superposition. Superposition of Sa2 molecules A, B, A' and B' with Sa and Sa3 structures gives an average r.m.s.d. of 0.69 Å, while the corresponding value for Sa2 molecule C is around 1.0 Å, reflecting the substantial conformational change in this molecule arising from the different orientation of Tyr87*C* and neighbouring residues. Analogous superpositions omitting residues 86–88 result in an average r.m.s.d. of 0.70 Å, which is in line with the other set of structures.

3. Results and discussion

3.1. Crystal form I

In form I there are three Sa2 molecules in the asymmetric unit, referred to as A, B and C, 277 water sites and a single sulfate anion at the active site of molecule A. There is a disulfide bond between cysteine residues 9 and 97. The peptide bond before Pro29 is in the *cis* conformation. The average temperature factors for main-chain atoms as a function of residue number are shown in Fig. 2. The differences in the variation of the B values for individual molecules are the result of different crystal contacts.

Least-squares overlap of all pairs of RNase Sa2 molecules (Table 3) based on 89 CA atoms shows that molecules A and B are closely similar to one another but molecule C is significantly different in the region around Tyr87 (see below). There are also deviations at the N-termini and loop 63–66, which were poorly defined in the density maps. The N-termini of molecules A and C form a tail pointing into the solution and are somewhat disordered. There is no electron density for the three N-terminal residues in molecule A and the N-terminal residue in molecule C and these were omitted from the model. In contrast, the N-terminus is well ordered in molecule B with clearly defined density as it is stabilized in a cleft between a segment of molecule B and neighbouring molecules in the crystal lattice. For residues 62–67 the typical electron density

Table 4
Residues modelled with two alternate conformations.

Form I			Form II	
A	*B*	*C*	*A*′	*B*′
Asn27	Asn33	Leu21	Asp7	Ala17
Val37	Arg34	Glu40	Arg34	Gln18
Asn51	Thr58		Asn65	Asp19
Arg96			Gln80	Thr20
			Gln91	

in the $(3F_o - 2F_c, \alpha_c)$ map is only about 0.5σ and for some atoms there is no electron density at all. Indeed, the loop was only modelled in molecule *A*; residues Gly63, Ser64 and Asn65 in molecule *B* and Gly63, Ser64, Asn65 and Asp66 in molecule *C* were omitted.

In addition, nine side chains were modelled with two alternate conformations (Table 4). The final model has good stereochemistry (Table 2). The Ramachandran plot (Ramakrishnan & Ramachandran, 1965) calculated by the program *PROCHECK* (Morris *et al.*, 1992) shows that 93.4, 97.1 and 95.5% residues of molecules *A*, *B* and *C*, respectively, are in the most favoured regions. The remainder are in the additionally allowed regions.

At the position where the phosphate group of the mononucleotides is located in the complexes with RNase Sa, electron density with a tetrahedral shape was found in molecule *A*, suggesting the presence of a sulfate or a phosphate anion. The identity of the anion remains unclear as both anions are present in the mother liquor, but from our previous studies (Sevcik *et al.*, 1996) it is very likely that it is a sulfate. The anion is held in position by favourable interactions with Glu56, His86, Tyr87 and four arginine residues: three from molecule *A* (34, 67 and 71) and a fourth from the neighbouring molecule *C* (45).

Tyr87*C* and surrounding residues are shown in electron density in Fig. 3. The contact region of the dimer formed by molecules *A* and *C* is shown in Fig. 4. Tyr87*A* and Tyr87*B* have the same conformation as in RNase Sa structures, while the location and conformation of Tyr87*C* is significantly different. For Tyr87*C*, the main-chain CA atom moves almost 5 Å relative to its position in molecules *A* and *B* (and Sa), whilst the OH group at the end of the side chain moves by 10 Å. The CA of the catalytic His86*C* moves by more than 1.5 Å and the side chain has a different orientation, but its imidazole ring ends up in approximately the same position as in molecules *A* and *B*. Tyr87*A* lies at the bottom of the active site, with only 8% of its surface accessible to solvent. Its OH group forms hydrogen bonds to the side chain of the catalytic Glu56*A* and the sulfate oxygen. In contrast, Tyr87*C* flips out of the active site so that its side chain would be about 45% accessible in the molecule isolated from the crystal lattice. However, in the crystal complex the insertion of Tyr87*C* into the active site of molecule *A* makes it almost totally buried, with only 4% of its surface accessible to solvent.

The solvent-accessible surface buried at the *A*/*C* dimer interface is 1164 Å^2, as calculated by the program *SURFACE*, which corresponds to 582 Å^2 of the 5900 Å^2 total surface of each isolated molecule. This is slightly above the minimum of 9% required for classification of a dimer as a protein complex according to the definition of Janin (1996). While it is evident that molecules *A* and *C* interact tightly through their active sites and can be structurally classified as a dimer, there is no evidence for any significant dimerization in solution. The dimer is presumed to form either during the crystallization process or to be present at a very low level in solution.

In Fig. 4 the 2′-GMP molecule is shown in the active site of molecule *A* based on its position in its complex with RNase Sa (Ševčík *et al.*, 1991). The aromatic ring of Tyr87*C* is positioned in a plane very close to that of the mononucleotide base and interacts with Tyr87*A* and Phe39*A*, which form the bottom of the active site. In addition, Tyr87*C* OH forms a hydrogen bond with the amide NH group of Arg42*A* similar to that formed by the O6 atom of mononucleotide bases in the complexes with RNase Sa (Sevcik *et al.*, 1991; Sevcik, Hill *et al.*, 1993; Sevcik, Zegers *et al.*, 1993). Molecules *A* and *C* are bound to one another in the crystal by 18 hydrogen bonds, four of them mediated by water molecules, and by the burial of Tyr87*C*. Thus, it is not surprising that the interaction between mole-

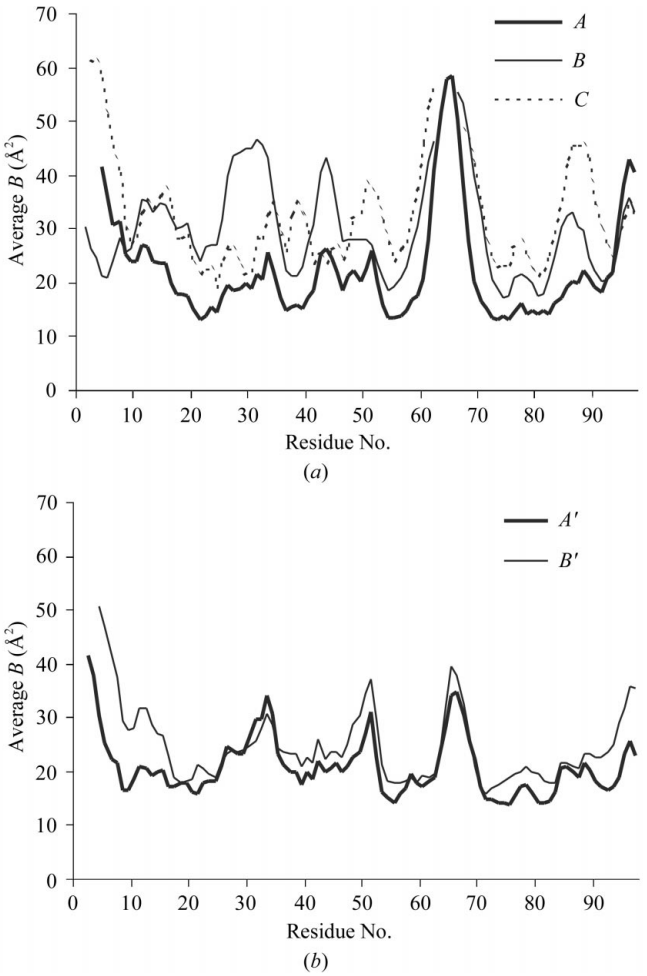

Figure 2
Average temperature factors as a function of residue number for structures I (*a*) and II (*b*).

cules *A* and *C* in the crystal is capable of providing the free energy necessary to stabilize the conformational change of molecule *C*.

The crystal packing of the molecules in form I requires the presence of one of the three independent RNase Sa2 molecules in a different conformation to that usually observed. The presence of the flipped-out Tyr87*C* conformation at a very low level in the solution population may be the reason behind the very slow growth of this crystal form. Such behaviour is certainly rarely encountered, but suggests that the packing of protein molecules in a crystal can occasionally trap conformations that are energetically less favourable but are present at very low levels in solution and that may be vital for function.

A classic example of this is the structure of the hormone glucagon (Sasaki *et al.*, 1975). The glucagon peptide is essentially unstructured in aqueous solution but takes up a helical conformation in the crystal, where it forms a trimer. The packing of the trimer interfaces is largely hydrophobic and it was proposed that this mimics the binding of the hormone to the membrane receptor *in vivo*. A similar conformational change occurs when the inhibitor IA, which is completely unfolded in solution, adopts an eight-turn helical structure in complex with proteinase A (Li *et al.*, 2000). These results confirm that interactions between protein molecules in a crystal can sometimes be strong enough to induce significant conformational changes of the interacting proteins or select conformations that exist at a low level in solution.

3.2. Crystal form II

In form II there are two enzyme molecules in the asymmetric unit, molecules *A*′ and *B*′, 171 water molecules and four sulfate ions. The refinement statistics are shown in Table 2.

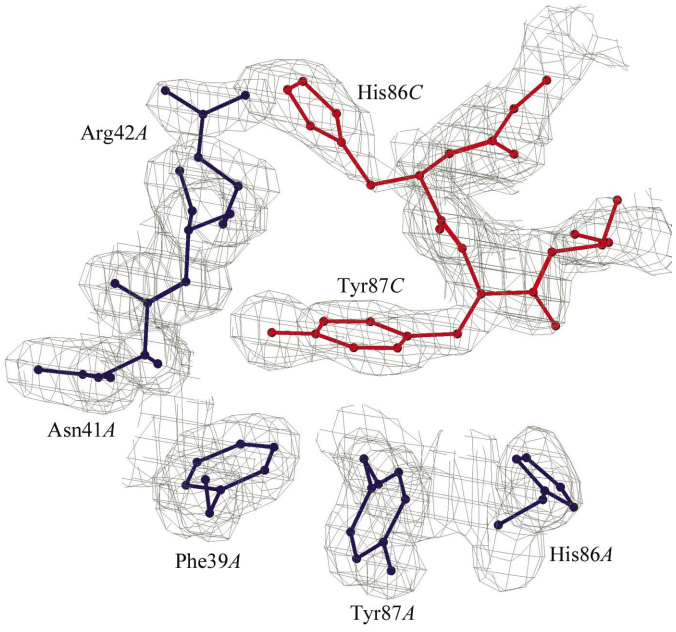

Figure 3
Tyr87*C* and the surrounding residues of molecule *A* in electron density contoured at the 1.0σ level using the program *BobScript* (Esnouf, 1999).

The Ramachandran plot shows that 100 and 98.6% of the residues of molecules *A*′ and *B*′, respectively, are in the most favoured region, with only one residue of molecule *B*′ in the additionally allowed region. The N-terminal residues are disordered: one residue is missing in molecule *A*′ and three in molecule *B*′. In contrast to form I, the loop 63–67 residues were well ordered in both molecules. The average temperature factors for main-chain atoms as a function of residue number are shown in Fig. 2.

Least-squares superposition of molecules *A*′ and *B*′ shows the largest difference at the CA atom of Gly63, which is caused by different crystal contacts influencing the conformation of this loop, which protrudes from the surface of the molecule. Molecules *A*′ and *B*′ are similar to form I molecules *A* and *B* but differ from *C* in the region around Tyr87 (Table 3).

Residues modelled with two alternate conformations are shown in Table 4. In molecule *B*′ residues 17–20, which form the central part of an α-helix, have two conformations for their main chain, with a maximum separation of 2.2 Å between CA

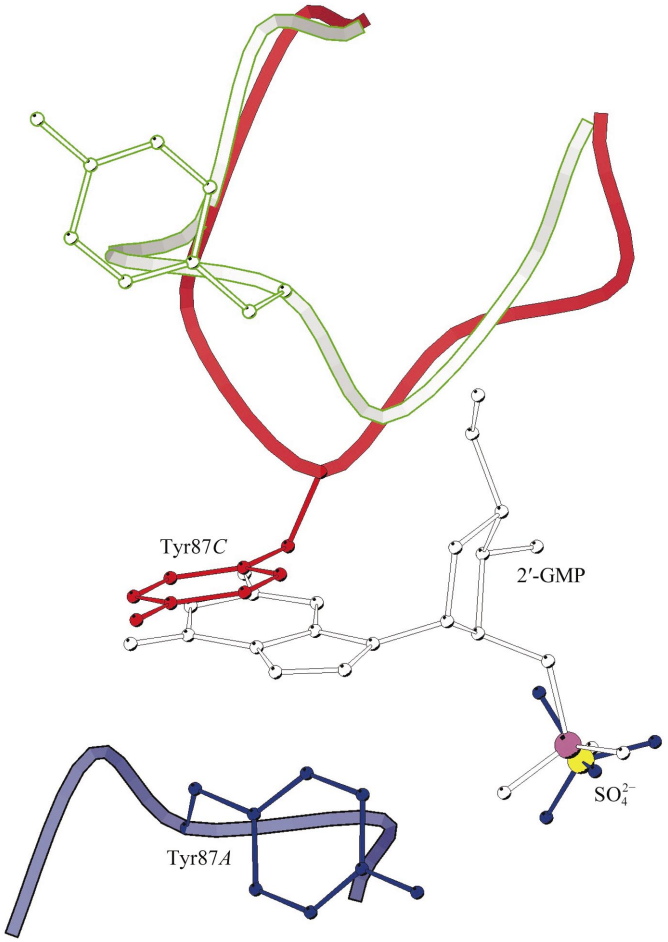

Figure 4
Flipped-out Tyr87C (red) inserted into the active site of molecule *A* (blue) in crystal form I. The green-coloured outlines show Tyr87*C* modelled in the usual conformation as seen in RNase Sa and in molecules *A* and *B* of Sa2. 2′-GMP was modelled into the active site of molecule *A* based on the structure of its complex with RNase Sa. The sulfate anion is located at the phosphate-binding site of molecule *A*. The figure was drawn using the program *MolScript* (Kraulis, 1991).

positions at Asp19. This double main-chain conformation was not seen in molecule A', probably owing to the different crystal environment.

In both A' and B' molecules there are two SO_4^{2-} ions. The first lies at the phosphate-binding site, where it forms a similar network of hydrogen bonds as in form I, the only difference being that in this case it is Arg42 of the neighbouring molecule that binds to the ion. The structures of RNase Sa2 as well as those of RNase Sa have shown that binding of a sulfate anion at the phosphate site strongly depends on the presence of an arginine residue from the neighbouring molecule, which makes an hydrogen bond with one of the sulfate O atoms. In the absence of the neighbouring molecule the ion does not bind. The second sulfate lies at the surface of the molecule, where it forms hydrogen bonds with Arg70 NH1 and NH2 and the main-chain N atoms of Ser15 and Gln16. The position of this ion suggests the localization of a substrate-binding subsite separated by several nucleotides from the active site.

4. Conclusions

The structure of RNase Sa2 is closely similar to that of Sa and Sa3, as Sa2 has 52% of its residues identical to both proteins. Fig. 5 shows a superposition of 41 molecules: 34 molecules of RNase Sa (resolution between 1.0 and 1.8 Å), five RNase Sa2 molecules and two Sa3 molecules (2.0 and 1.7 Å resolution). At first sight, this might be viewed as having some similarity to an ensemble of NMR structures. Each of the structures in this superposition is derived directly from experimental X-ray data and the coordinate accuracy varies from 0.05 Å in the atomic resolution structures of Sa to around 0.12 Å in the present structures for the well ordered parts of the molecules, which covers essentially all of the backbone. Thus, there is an intrinsic error in the coordinates and one would expect some variation between the 41 molecules. The variation evident in Fig. 5 has four major components: (i) the intrinsic experimental error, which should have a normal distribution with r.m.s. differences around 0.1 Å, (ii) differences caused by the various crystallization conditions and the packing in the various crystal forms, (iii) differences caused by the formation of complexes with nucleotides and barstar and (iv) differences arising from the amino-acid substitutions between the three enzymes.

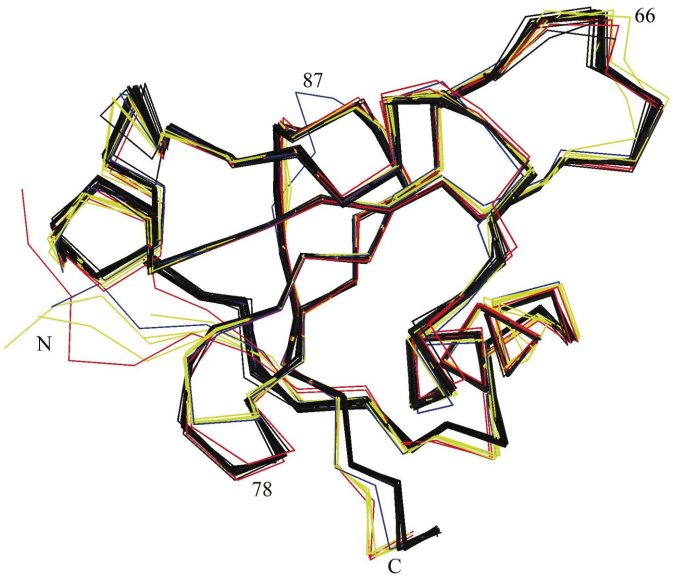

Figure 5
Overlap of the structures of five Sa2 molecules (yellow, except molecule *C* which is in blue), two Sa3 molecules (red) and 34 Sa molecules (black) based on the superposition of 89 corresponding CA atoms.

It is immediately obvious that the core of the enzyme, including the major part of the main chain, is a rather rigid unit and varies little between all these molecules. The regions where there is a substantial deviation between structures lie on the surface of the fold. It can be seen that there is substantial flexibility in the N-termini and indeed these residues are poorly defined in several of the structures (Sa2 and Sa3). The C-termini show some variation in conformation, but much less than that of the N-termini, as the very last residue in each molecule, which is a cysteine, makes a disulfide bridge with the other cysteine. The loops around residue 66 vary in all structures owing to crystal packing. There is a relatively large deviation between Sa2 and the other structures around Thr78 (Sa numbering) as there is one deletion in the Sa2 sequence.

The major deviant loop around Tyr87 in molecule *C* of RNase Sa2 is a clear outlier in this superposition. It arises from the flipped main chain. Molecule *C* form I shows substantial conformational changes in the active site not only in comparison with the other four Sa2 molecules in forms I and II but also with all Sa and Sa3 structures. Sa2 molecules *A* and *C* form an asymmetric dimer in the crystal, with the two molecules interacting through their active sites by a number of hydrogen bonds to form a species which must be catalytically inactive as the active sites are buried; this can be treated as an example of self-inhibition in the crystal dimer. However, there is no evidence that there are stable complexes of this type in solution. This may arise from either the formation of a transient dimer in solution, with one of the two molecules having its Tyr87 in the flipped-out conformation, or during the actual packing of molecules onto the nascent crystal surface. In either case, the presence of the flipped-out conformation at a low level is required for the recognition between molecules *A* and *C* and for the formation of a dimer in the crystal.

The aromatic ring of the flipped-out active site Tyr87 of molecule *C* is positioned at the substrate-binding site of molecule *A*. The plane of the aromatic ring is very close to the plane in which the guanosine base is situated in the mononucleotide inhibitor complexes with RNase Sa. The phosphate-binding site of one of the two interacting molecules is occupied by a sulfate anion, which forms a similar hydrogen-bond network to the phosphate group of the substrate. The significance of the flipped-out active-site Tyr87 in molecule *C* of Sa2 is not clear. Whether this is just an artefact of the crystal form or whether the conformation is relevant to the function of the enzyme requires further study. All crystals of Sa and Sa2 obtained to date have been grown under virtually the same conditions of temperature, pH, salt and protein concentration. This shows that the packing of protein molecules in a crystal

can occasionally trap a conformation which is energetically less favourable and probably present at very low levels in solution. For Sa2, the relatively high salt concentration in the crystallization solution may have promoted the formation of the dimer, favouring hydrophobic interactions between the active-site residues of the two molecules.

Taking into account the mobility of the loop around Tyr87 in form I and the two main-chain conformations observed in the α-helix of one molecule in form II, the flexibility of the surface loops owing to crystal contacts in the structures of RNase Sa2, RNase Sa (Sevcik *et al.*, 1991) and RNase Sa3 (Ševčík, Urbanikova *et al.*, 2002), together with the flexibility of the segments showing open and closed conformations of the active site in RNase Sa (Ševčík, Lamzin *et al.*, 2002), it can be concluded that *Streptomyces* ribonucleases possess substantial flexibility. This is surprising as the enzymes are relatively stable and the crystals diffract to high resolution (0.85 Å in the case of Sa, unpublished results). This confirms the view that structures determined by X-ray diffraction, often considered to be rigid folds, have substantial flexibility in some regions of the protein molecules comparable to that suggested by NMR.

The authors thank the EMBL in Hamburg for providing facilities on beamline X31 and Dr Fred Antson from the University of York for measuring the data for crystal form II. This research was supported by grants awarded by Howard Hughes Medical Institute (grant No. 75195-547601) and by the Slovak Academy of Sciences (grant No. 2/1010/96).

References

Brünger, A. T. (1993). *Acta Cryst.* D**49**, 24–36.
Collaborative Computational Project, Number 4 (1994). *Acta Cryst.* D**50**, 760–763.
Esnouf, R. M. (1999). *Acta Cryst.* D**55**, 938–940.
Hartley, R. W., Both, V., Homerova, D., Jucovic, M., Nazarov, V., Rybajlak, I. & Sevcik, J. (1996). *Protein Pept. Lett.* **4**, 225–231.
Hebert, E. J., Grimsley, G. R., Hartley, R. W., Horn, G., Schell, D., Garcia, S., Both, V., Sevcik, J. & Pace, C. N. (1997). *Protein Expr. Purif.* **11**, 162–168.
Janin, J. (1996). *Proteins*, **25**, 438–445.
Jones, T. A. (1978). *J. Appl. Cryst.* **11**, 268–272.
Kraulis, P. J. (1991). *J. Appl. Cryst.* **24**, 946–950.
Leland, P. A. & Raines, R. T. (2001). *Chem. Biol.* **8**, 405–413.
Li, M., Phylip, L. H., Lees, W. E., Winther, J. R., Dunn, B. M., Wlodawer, A., Kay, J. & Gustchina, A. (2000). *Nature Struct. Biol.* **7**, 113–117.
McRee, D. E. (1993). *Practical Protein Crystallography*. San Diego: Academic Press.
Matthews, B. W. (1968). *J. Mol. Biol.* **33**, 491–497.
Morris, A. L., MacArthur, M. W., Hutchinson, E. G. & Thornton, J. M. (1992). *Proteins*, **12**, 345–364.
Murshudov, G. N., Vagin, A. & Dodson, E. J. (1997). *Acta Cryst.* D**53**, 240–255.
Navaza, J. (1994). *Acta Cryst.* A**50**, 157–163.
Otwinowski, Z. & Minor, W. (1997). *Methods Enzymol.* **276**, 307–326.
Perrakis, A., Morris, R. M. & Lamzin, V. S. (1999). *Nature Struct. Biol.* **6**, 458–463.
Ramakrishnan, C. & Ramachandran, G. N. (1965). *Biophys. J.* **5**, 909–933.
Sasaki, K., Dockerill, S., Adamiak, D. A., Tickle, I. J. & Blundell, T. (1975). *Nature (London)*, **257**, 751–757.
Sevcik, J., Dauter, Z., Lamzin, V. S. & Wilson, K. S. (1996). *Acta Cryst.* D**52**, 327–344.
Sevcik, J., Dodson, E. J. & Dodson, G. G. (1991). *Acta Cryst.* B**47**, 240–253.
Sevcik, J., Hill, C. P., Dauter, Z. & Wilson, K. S. (1993). *Acta Cryst.* D**49**, 257–271.
Ševčík, J., Lamzin, V. S., Dauter, Z. & Wilson, K. S. (2002). *Acta Cryst.* D**58**, 1307–1313.
Ševčík, J., Urbanikova, L., Leland, P. A. & Raines, R. T. (2002). *J. Biol. Chem.* **277**, 47325–47330.
Sevcik, J., Zegers, I., Wyns, L., Dauter, Z. & Wilson, K. S. (1993). *Eur. J. Biochem.* **216**, 301.